

# Tandem reductive catalytic upgrading of orange peel waste derived methyl levulinate and limonene into $\gamma$ -valerolactone and *p*-cymene promoted by Pd/ZrO<sub>2</sub> and ZrO<sub>2</sub> catalysts

A. Allegri<sup>a</sup>, E. Paone<sup>b,c,\*</sup>, C. Bosticco<sup>a</sup>, A. Pedullà<sup>b</sup>, M.G. Musolino<sup>b</sup>, F. Cavani<sup>a,c</sup>, T. Tabanelli<sup>a,c,\*\*</sup>, S. Albonetti<sup>a,c</sup>

<sup>a</sup> Dipartimento di Chimica Industriale "Toso Montanari", Università di Bologna, Viale Risorgimento 4, Bologna I-40136, Italy

<sup>b</sup> Dipartimento di Ingegneria Civile, dell'Energia, dell'Ambiente e dei Materiali (DICEAM), Università Degli Studi "Mediterranea" di Reggio Calabria, Loc. Feo di Vito, Reggio Calabria I-89122, Italy

<sup>c</sup> Consorzio Interuniversitario per la Scienza e la Tecnologia dei Materiali (INSTM), Firenze 50121, Italy

## ARTICLE INFO

### Keywords:

Orange peel waste  
Dehydrogenation  
Catalytic transfer hydrogenation  
Methyl levulinate  
 $\gamma$ -valerolactone  
Limonene  
*p*-cymene  
Zirconia  
Palladium

## ABSTRACT

Orange peel waste (OPW), a significant biomass byproduct derived from the juice processing industry, can be used as valuable resource to produce various chemicals, including methyl levulinate (ML) and limonene (LIM). This study introduces a tandem catalytic process involving the dehydrogenation of LIM into *p*-cymene and the (transfer) hydrogenation of ML into  $\gamma$ -valerolactone (GVL), unlocking the full potential of OPW chemo-catalytic valorisation in the spirit of circular economy. This process is promoted by the heterogeneous Pd/ZrO<sub>2</sub> and *t*-ZrO<sub>2</sub> catalysts in the presence of ethanol as hydrogen-donor solvent. Under batch conditions, Pd/ZrO<sub>2</sub> not only shows superior performance in the transfer hydrogenation of ML compared to *t*-ZrO<sub>2</sub>, but also promotes the conversion of LIM into *p*-cymene primarily through the hydrogenation/dehydrogenation route. Most important, Pd/ZrO<sub>2</sub> exhibits good activity in the simultaneous upgrading of both ML and LIM across various ML:LIM ratios.

Continuous gas-flow conditions result in improved outcomes in terms of ML and LIM conversion, as well as GVL and CYM selectivity. Notably, a strong correlation between CYM and H<sub>2</sub> yields has been established providing compelling evidence for the LIM isomerization-dehydrogenation pathway. However, the simultaneous upgrading of LIM and ML was found to be not efficient in the gas-phase due to side oligomerization reactions.

## Introduction

Lignocellulosic biomasses, including biomass-derived wastes and residues, are readily available feedstocks for producing value-added chemicals, pharmaceuticals, biofuels, and renewable energy [1–3]. The chemo-catalytic valorization of non-edible lignocellulosic losses of agri-food industries is particularly challenging since such materials have a complex chemical composition that includes many valuable compounds (e.g. minerals, vitamins, acids, crude proteins, etc.), in addition to lignocellulose.

Citrus fruits make up nearly 18 % of the total fruit production, and oranges, being the most produced globally, account for 60 % of this citrus yield. Brazil tops global orange production with 17.1 Mton annually, followed by China (10.6 Mton), India (9.5 Mton) and the

United States (4.8 Mton), contributing to a total of 78.7 Mton worldwide. In 2017, the EU Member States collectively harvested 6.1 Mton of oranges. Spain contributed over half, with 3.2 Mton (52 % of the EU total), followed by Italy at 1.5 Mton (25 %) and Greece at 0.9 Mton (15 %) [4]. The juice industry worldwide predominantly manufactures orange juice, which is consumed in significant quantities. Orange peel waste (OPW) represents an abundant biomass food loss generated in huge amounts every year by the juice processing industry which produced over 50 million metric tons in 2020 [5]. OPW has big potential as renewable starting material to produce chemicals and energy due to its high content of sugars, antioxidants, and essential oils (mainly limonene). Through various processes – including extraction, pyrolysis, hydrothermal carbonization, anaerobic digestions, fermentation, and many others – OPW can be converted into value-added products such as

\* Corresponding author at: Consorzio Interuniversitario per la Scienza e la Tecnologia dei Materiali (INSTM), Firenze 50121, Italy.

\*\* Corresponding author at: Dipartimento di Chimica Industriale "Toso Montanari", Università di Bologna, Viale Risorgimento 4, Bologna I-40136, Italy.

E-mail addresses: [emilia.paone@unirc.it](mailto:emilia.paone@unirc.it) (E. Paone), [tommaso.tabanelli@unibo.it](mailto:tommaso.tabanelli@unibo.it) (T. Tabanelli).

<https://doi.org/10.1016/j.mcat.2024.113840>

Received 26 December 2023; Received in revised form 11 January 2024; Accepted 11 January 2024

Available online 30 January 2024

2468-8231/© 2024 The Author(s). Published by Elsevier B.V. This is an open access article under the CC BY-NC-ND license (<http://creativecommons.org/licenses/by-nc-nd/4.0/>).

biofuels, platform chemicals and natural flavoring agents [6–10]. The holocellulose fraction (cellulose and hemicellulose) of dry OPW can account for up to 50 % and can be employed as a renewable source of C6–C5 sugars, alcohols/polyols, as well as furan and levulinate derivatives [11–13]. Methyl-levulinate (ML), now easily obtainable directly from OPW [7,14], finds several applications including fuel additives, flavoring agents, and raw intermediates for the preparation of plasticizers, coatings, adhesives, and pharmaceuticals. The catalytic reduction of ML allows the production of  $\gamma$ -valerolactone (GVL), which is a well-known, non-toxic, biobased solvent that has drawn considerable attention as an important precursor for industrial chemistry [14–19]. The global GVL market reached a size of nearly 640 million EUR in 2022, and projections suggest it will exceed 780 million EUR by 2031, reflecting a Compound Annual Growth Rate (CAGR) of 2.24 % [20]. The use of methyl levulinate in the preparation of GVL is gaining significant attention due to the lower boiling point and free acid characteristics of alkyl levulinates if compared to levulinic acid (one of the 12 bio-based molecules that in the near future can replace petroleum-based chemicals) [18,19]. Additionally, alcoholic groups in alkyl levulinates act as better leaving groups than OH, which facilitates the formation of GVL through an intramolecular cyclization mechanism. Considering the potential applications of GVL in the bio-based economy, there is an increasing need for sustainable and cost-effective processes for its production, starting from biobased alkyl levulinates.

One of the most sustainable approaches for the conversion of ML into GVL is the catalytic transfer hydrogenation (CTH) process through the Meerwein-Ponndorf-Verley (MPV) reaction, in which H-donor solvents can be adopted as an indirect H-source. The CTH of ML into GVL can be promoted both in the presence or in absence precious metal catalysts. To this regard, high surface area tetragonal zirconia ( $t$ -ZrO<sub>2</sub>) seems to be one of the most active and selective system being able to promote a series of reactions including the carbonyl CTH reduction and successive cyclisation to GVL and/or direct intramolecular cyclization into  $\alpha$  and  $\beta$  angelica lactones that can be further reduced into GVL [16–18]. Noteworthy, this reaction can be performed also under continuous-flow, gas-phase conditions, as recently reported by our groups [18,19]. In this case, a careful design of the catalyst properties is of pivotal importance to limit undesired alkylation (i.e. due to the activation of co-produced methanol), ketonisation and oligomerization reactions [21–25].

The use of an indirect H-source in hydrogenation and hydrogenolysis reactions is becoming progressively important in industrial processes due to its ability to address the limitations associated with high-pressure molecular hydrogen, such as the high costs of purchase, transport, and infrastructure, as well as safety concerns [25,26]. By utilizing renewable feedstocks to generate hydrogen-donor molecules, such as alcohols and terpenes, these reactions can be carried out under milder conditions, which reduces the need for expensive equipment and costly infrastructure. This approach not only enhances the sustainability of the process but also promotes the development of a bio-based economy that relies on renewable feedstocks for the production of valuable chemicals and fuels.

In this context, limonene – the main constituent of citrus essential oil – was recently used as an H-donor source for the deoxygenation of fatty acids into alkanes and arenes or in the upgrading of palm oil into bio-jet fuel [27,28]. This approach is worth of investigation since limonene can be readily extracted from orange peel waste, which is a rich and abundant source of this compound, thus providing an eco-friendly and sustainable alternative to classical H-donor molecules/solvents (simple primary and secondary alcohols, formic acid, NaBH<sub>4</sub> decalin, tetralin, polymethylhydrosiloxane).

Therefore, in this contribution, we decided to investigate the use of limonene as an alternative hydrogen-donor molecules in the transfer hydrogenation of methyl levulinate into GVL both under batch and continuous gas-flow conditions by using  $t$ -ZrO<sub>2</sub> and Pd/ZrO<sub>2</sub> catalysts with the final aim to highlights the circular economy potential of

utilizing OPW-derived feedstocks in catalytic processes.

The catalytic results underscore the efficacy of the Pd/ZrO<sub>2</sub> catalyst in promoting tandem reductive catalytic upgrading of ML and LIM under both batch and continuous flow conditions, providing valuable insights into reaction mechanisms, temperature and time effects, and the interplay of reactant ratios for optimizing the overall process efficiency.

## Experimental section

### Catalysts preparation and characterization

The analytical grade chemicals were obtained from commercial sources (Sigma Aldrich, Alfa Aesar and CARLO ERBA Reagents) and were used without further purification.

High specific surface area (SSA)  $t$ -ZrO<sub>2</sub> was synthesized optimizing a previously reported procedure [17,29]. Briefly, a 0.3 M aqueous solution of ZrO(NO<sub>3</sub>)<sub>2</sub> • 2H<sub>2</sub>O (Aldrich, purity 99 %) was added dropwise to a 5 M NH<sub>3</sub> solution at room temperature, with a Zr/NH<sub>3</sub> ratio of 1/10. The resulting mixture was digested at reflux for 48 h, keeping a constant pH of 9 via continuous addition of a concentrated NH<sub>3</sub> solution (28% wt) with a syringe pump (KDSscientific Legacy Syringe-infusion Pump). The precipitate was filtered and washed several times, still using a NH<sub>3</sub> (3 M) solution and dried overnight at 120 °C and calcined at 500 °C for 12 h in flowing air with a heating rate of 5 °C/min. The resulting material was either used directly as  $t$ -ZrO<sub>2</sub> or employed for the synthesis of the Pd/ZrO<sub>2</sub> catalyst. The addition of Pd was achieved via incipient wetness impregnation by adding a solution of palladium(II) acetylacetonate (Aldrich, purity 99 %) dissolved in acetone to the support. After impregnation, Pd/ZrO<sub>2</sub> was dried for 1 day under vacuum at 100 °C and, before its use in catalytic reactions, reduced at 300 °C for 2 h under a flow of hydrogen (1 cc/min).

The BET surface area was determined by the single-point BET technique at –196 °C (77 K) using N<sub>2</sub> adsorption-desorption isotherms, after outgassing under flowing nitrogen for 1 h at 150 °C, using a Fisons Sorpity 1750 instrument.

XRD analyses were conducted using the Ni-filtered Cu K $\alpha$  radiation ( $\lambda = 1.54178 \text{ \AA}$ ) on a Philips X'Pert vertical diffractometer equipped with a pulse height analyser and a secondary curved graphite-crystal monochromator.

NH<sub>3</sub> and CO<sub>2</sub>-TPD analyses were performed with a Micromeritics AutoChem II 2920 instrument equipped with a TCD. The fresh catalyst was pre-treated in He at 500 °C, followed by cooling down to 40 °C for CO<sub>2</sub>-TPD and 100 °C for NH<sub>3</sub>-TPD. The catalyst surface was saturated with CO<sub>2</sub> or NH<sub>3</sub> for 1 h and then the physically adsorbed probe molecule was removed by flushing the sample with He. The NH<sub>3</sub> adsorption was conducted at 100 °C to eliminate the contribution of weak acid sites. The temperature-programmed desorption was followed via TCD, by increasing the temperature at a constant rate of 10 °C/min from 40/100 °C to 500 °C in He.

### Catalytic tests

Catalytic tests under batch conditions were performed at 500 rpm in a 100 mL stainless steel reactor (Parr Instrument - 4560 Mini reactor system). The reactor was loaded with the catalyst (0.3 g) suspended in a 10% wt alcoholic solution (MeOH, EtOH, 2-PrOH) containing the chosen substrate(s). Any trace of air present in the system was eliminated by fluxing three times N<sub>2</sub> (99.99 %). The reactor was subsequently pressurized with 10 bar of desired input gas and heated at the final reaction temperature. At the end of the reaction, the system was cooled down at room temperature, the pressure carefully released, and the analysis of the organic phase was done by using an off-line gas-chromatograph.

Gas-phase catalytic tests were carried out in a continuous-flow fixed-bed micro-reactor (Pyrex, length of 38 cm, internal diameter of 85 mm). 1 mL of catalyst (30–60 mesh particles) was placed in the reactor, and then it was heated to the desired reaction temperature under N<sub>2</sub> flow (16

NmL min<sup>-1</sup>). The catalytic reaction was started by the vaporization of the reactants using N<sub>2</sub> as the carrier gas (15 NmL min<sup>-1</sup>). Limonene (racemic mixture, 95 % purity, Aldrich) or methyl levulinate (98 % purity, Aldrich) were employed as reactants, either neat or dissolved in ethanol (99.8 % purity, Aldrich) with a molar ratio of reactant to ethanol of 1:10. The total volumetric flow rate through the catalytic bed was held constant at 60 mL min<sup>-1</sup> and the organic (i.e. LIM, ML and ethanol) content of the gas flow was kept at 1 % for the reactions without ethanol and between 8 % and 9 % for the reactions with ethanol. Analyses of reactants and products were carried out as follows: the outlet stream was scrubbed for 1 h in acetonitrile. 20 µL of n-octane were added to the acetonitrile solution with the condensed products (ML, Ethyl Levulinate (EL), GVL, Ethyl Pentenoate (EPE), Ethyl Pentanoate (EPA), LIM, Menthenes (MTE), Menthanes (MTA), Terpinenes (TER) and CYM). 0.5 µL of this solution were then analyzed using a PerkinElmer Clarus 500 Gas Chromatograph equipped with an Agilent HP-5 capillary column (25 m x 320 µm x 0.25 µm) and a Flame Ionization Detector (FID). The carrier used was N<sub>2</sub> with a flow of 1.2 mL/min. The heating program used was the following: 2 min isotherm at 50 °C, then heating up to 110 °C with a rate of 10 °C/min and later maintained for 2 min. finally, heating up to 250 °C with a heating rate of 15 °C/min and then maintained for 2 min. H<sub>2</sub> production was analyzed on-line after scrubbing of condensed products with a PerkinElmer Clarus 500 Gas Chromatograph equipped with a TCD detector and a Carbosphere® 80/100 mesh column., using 45 mL/min of N<sub>2</sub> as carrier at a constant temperature of 95 °C. External calibration method was used for the identification and quantification of reactants and products, using reference commercial samples.

The conversion, product selectivity and product yield were defined and calculated as:

$$(1) \text{ Conversion (\%)} = \frac{\text{mol reacted substrate}}{\text{mol of substrated feed}} \times 100$$

$$(2) \text{ Liquid phase selectivity (\%)} = \frac{\text{mol of specific product in liquid phase}}{\text{sum of mol of all products in liquid phase}} \times 100$$

$$(3) \text{ Product yield (\%)} = \frac{\text{mol of specific product}}{\text{mol of substrated feed}} \times 100$$

For the gas phase reaction, the  $\Sigma Y/X$  value was calculated as a ratio between the sum of the yields of all the products deriving from a reactant and that reactant's conversion. In particular,

$$(1) \frac{\Sigma Y}{X}_{ML} = \frac{Y_{EL} + Y_{GVL} + Y_{EPE} + Y_{EPA}}{X_{ML}}$$

$$(2) \frac{\Sigma Y}{X}_{LIM} = \frac{Y_{MTE} + Y_{MTA} + Y_{TER} + Y_{CYM}}{X_{LIM}}$$

The identification of products was performed by comparison with commercially available samples and by means of a GC-MS equipped with a non-polar column HP-5 (95 % dimethylsiloxane and 5 % phenyl, 30 m x 320 µm, using the same heating program as reported for the GC-FID analysis), coupled with a mass spectrometer (Agilent Technologies 5973 inert).

## Results and discussion

### Catalysts synthesis and characterization

Table 1 presents the main characteristics and structural properties of investigated Pd/ZrO<sub>2</sub> and t-ZrO<sub>2</sub> catalysts.

Although physical-chemical features of the t-ZrO<sub>2</sub> catalyst have been extensively discussed in various reports [30,31], including some of the authors [17,32]; the optimization of the synthetic procedure of t-ZrO<sub>2</sub> herein reported, specifically the digestion step and the careful control of pH for more than 48 h, yielded significant improvements upon the previously reported materials [17,29]. These improvements can be summarized as follows: (i) the XRD pattern suggested a nanocrystalline tetragonal phase (Fig. 1); (ii) a high surface area of 250 m<sup>2</sup>/g indicated

**Table 1**

Main characteristics of the investigated catalysts (SA = surface area as determined by BET analysis; acid density as determined via NH<sub>3</sub>-TPD analysis; base density as determined via CO<sub>2</sub>-TPD analyses; Pd loading and average particle size by TEM-EDX).

Catalyst notation	SA [m <sup>2</sup> /g]	acid density [mmol/g NH <sub>3</sub> desorbed]	base density [mmol/g CO <sub>2</sub> desorbed]	Pd loading [%]	Average Pd particle size [nm]
Pd/ZrO <sub>2</sub>	138	0.59	0.030	5	1,25
t-ZrO <sub>2</sub>	250	0.57	0.105	–	–

by BET measurement, and (iii) a higher density of acidic sites, expressed as mmol of desorbed ammonia per gram of catalyst, demonstrated by NH<sub>3</sub>-TPD (for comparison a 120 m<sup>2</sup>/g t-ZrO<sub>2</sub>, was characterized by 0.49 mmol/g NH<sub>3</sub>).

XRD spectra of Pd/ZrO<sub>2</sub>, after the reduction with H<sub>2</sub> at 300 °C, is reported in Fig. 1–left side. The features resemble closely those of the support, with two broad peaks ascribable to the convolution of the four main peaks of tetragonal zirconia (JCPDS 17–0923). The broad nature of the characteristic XRD peaks, along with the TEM images and a preliminary Scherrer calculation, suggest a t-ZrO<sub>2</sub> crystallite size below 3 nm. On the other hand, the absence of the (1 1 1) diffraction line of metallic palladium is indicative of extremely small highly dispersed Pd-particles as confirmed by TEM analysis that reveals an average particle size of 1.25 nm with a narrow particle size distribution of with a majority of 1 nm diameter particles (Fig. 1–right).

### Catalytic tests under batch conditions

Under liquid phase and batch conditions, to expedite the screening of catalysts and to obtain initial insights into the temperature effect, Pd/ZrO<sub>2</sub> and t-ZrO<sub>2</sub> catalysts were explored in the transfer hydrogenation of methyl levulinate by using ethanol as indirect H-source in the temperature range of 200–300 °C (Table 2).

The transfer hydrogenation of alkyl levulinates with alcohols to produce  $\gamma$ -valerolactone (GVL) has been extensively documented, especially in liquid phase [33,34]. In a simplified context, when ethanol (EtOH) is used as a solvent and hydrogen donor, alkyl levulinates (ML) can engage in a sequence of reported reactions, summarized in Scheme 1, encompassing: (i) cyclization into angelica lactones (AnL), followed by subsequent reduction into GVL, and/or (ii) transesterification of ML, AnL or GVL with ethanol leading to the formation of either ethyl levulinate (EL) or the corresponding ethyl 4-hydroxypentanoate; and/or (iii) direct CTH of the ML or EL carbonyl to give the corresponding hydroxy-esters which can then undergo intramolecular cyclisation to GVL or have the potential for further conversion into pentenoates (i.e. ethylpentenoate EPE) and pentanoates (i.e. ethylpentenoate, EPA).

After 6 h of reaction, a substantial ML conversion of 73 % at 300 °C can be achieved when utilizing Pd/ZrO<sub>2</sub> as catalyst, resulting in an overall GVL yield of 24 %. The sole additional reaction product identified was ethyl levulinate (EL) mainly ascribable to the transesterification reaction of ML with EtOH. As expected, lower temperatures (200 and 250 °C) led to minor conversions, accompanied by a notable shift in product selectivity as a consequence of the higher tendency of ML to undergo a transesterification process under the adopted reaction conditions.

Reactions performed in the presence of t-ZrO<sub>2</sub> exhibited a somewhat reduced efficiency in GVL production with a more marked inclination in promoting the transesterification reaction.

The time effect on the conversion of ML and GVL yield was investigated at 250 °C and reported in Fig. 2. In the case of Pd/ZrO<sub>2</sub> catalyst, the ML conversion progressively increases from 14 % at 3 h to 35 % at 6 h and reaching 68 % after 24 h of reaction time with the pattern of products appearing almost unchanged. Also in this case, a negligible amount (approximately 1 %) of side-products was registered only after

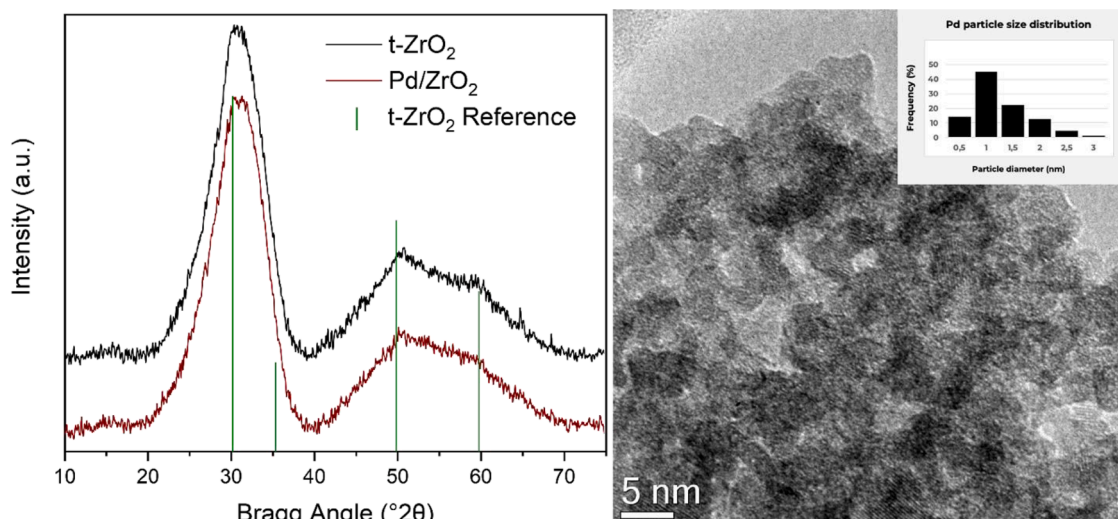


**Fig. 1.** Left side: XRD patterns of *t*-ZrO<sub>2</sub> and Pd/ZrO<sub>2</sub> catalysts compared with the tetragonal zirconia reference (JCPDS 17–0923). Right Side: high-resolution transmission electron micrograph of the of the Pd/ZrO<sub>2</sub> catalyst (inset: size distribution of the palladium nanoparticles).

**Table 2**

Catalyst screening and reaction temperature effect in the transfer hydrogenation of methyl levulinate in the presence of Pd/ZrO<sub>2</sub> or *t*-ZrO<sub>2</sub> catalyst by using ethanol as H-source.

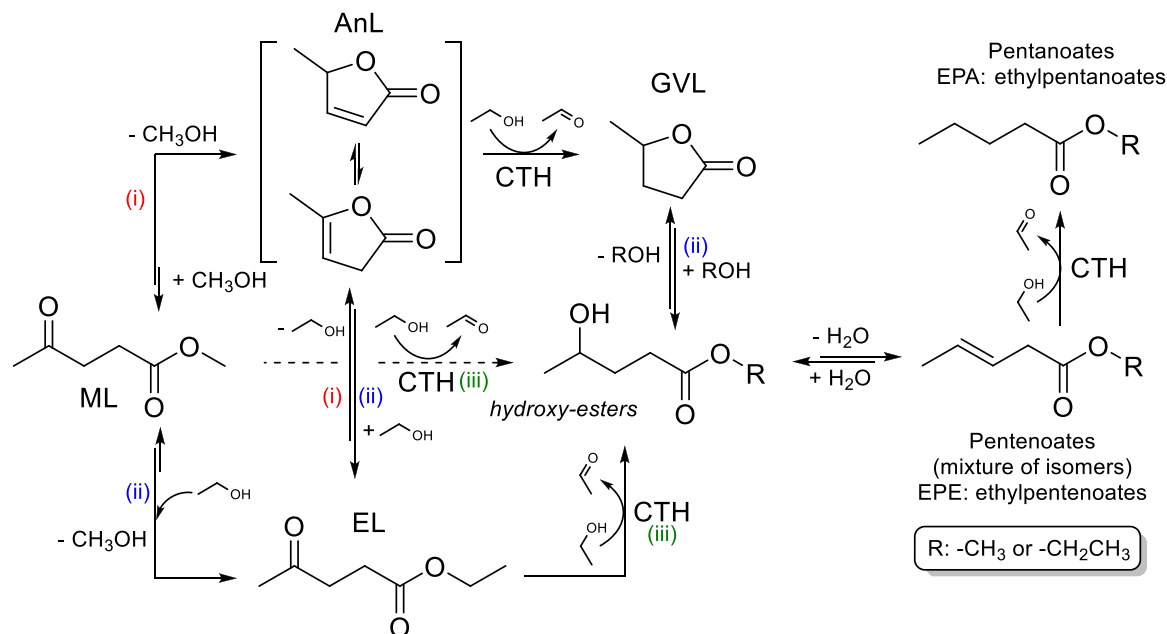
Catalyst	Temperature [°C]	Conversion [%]	Liquid Product Selectivity [%]		GVL Yield [%]
			GVL	EL	
Pd/ZrO <sub>2</sub>	300	76	43	57	33
Pd/ZrO <sub>2</sub>	250	35	40	60	14
Pd/ZrO <sub>2</sub>	200	21	23	77	5
<i>t</i> -ZrO <sub>2</sub>	300	73	33	67	24
<i>t</i> -ZrO <sub>2</sub>	250	32	17	83	6
<i>t</i> -ZrO <sub>2</sub>	200	10	9	90	1

GVL:  $\gamma$ -valerolactone; EL: ethyl-levulinate; [reaction conditions: 40 mL of methyl levulinate solution in EtOH (10% wt); 0.2 g of catalyst; initial N<sub>2</sub> pressure: 10 bar; reaction time: 6 h; speed stirring: 500 rpm.]

24 h of reaction time. A similar pattern, characterized by lower ML conversion across all investigated reaction times, is noted with the *t*-ZrO<sub>2</sub> catalyst.

The cumulative findings on temperature and time effects unequivocally indicate that the introduction of palladium into the *t*-ZrO<sub>2</sub> system has a negligible impact on ML conversion. In contrast, it significantly enhances the activation of ethanol and the consequent transfer hydrogenation reaction compared to the transesterification, thus directing the product selectivity towards increased GVL production. In none of the reactions AnL have been detected, either in traces. This evidence, together with the literature on the CTH of alkyl levulinate with alcohols in liquid phase [33,35], support the hypothesis that, in these conditions, Pd/ZrO<sub>2</sub> mainly promotes the direct reduction of the alkyl levulinates carbonyl to the corresponding hydroxy-esters which rapidly undergoes to intramolecular cyclisation forming GVL.

The effect of solvent/H-donor was also investigated, and results are sketched in Fig. 3. Reactions conducted in the presence of MeOH



**Scheme 1.** Simplified reaction scheme of methyl levulinate (ML) reduction via CTH with ethanol to GVL or Ethyl Levulinates and their further conversion into pentenoates (EPE) and pentanoates (EPA).

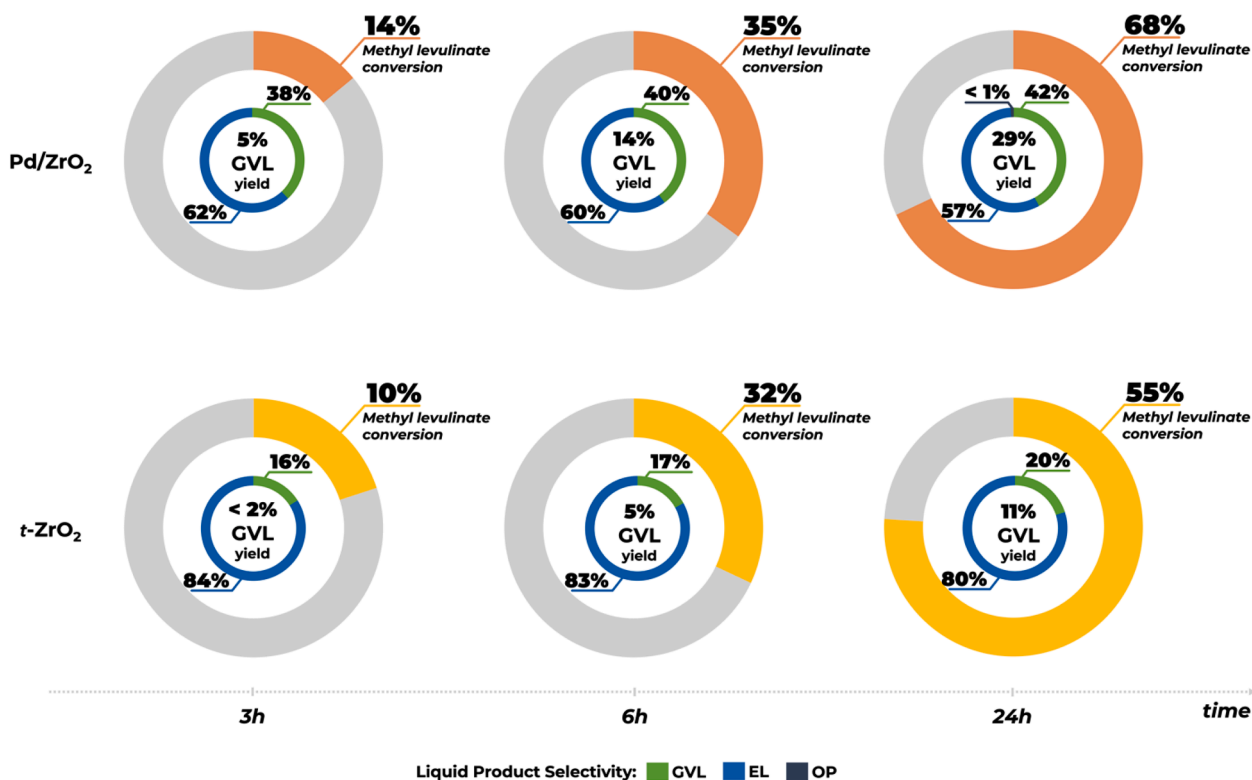


Fig. 2. Time effect in the transfer hydrogenation of methyl levulinate in the presence of Pd/ZrO<sub>2</sub> or t-ZrO<sub>2</sub> catalyst by using ethanol as H-source at 250 °C (GVL:  $\gamma$ -valerolactone; EL: ethyl-levulinate; OP: other products).

exhibited near inactivity with both catalytic systems. In the presence of 2-PrOH, marginally improved outcomes, specifically in terms of ML conversion, were observed compared to EtOH. This outcome can be easily attributed to the well-established higher propensity of secondary alcohols to release hydrogen. On the other hand, reactions carried out in the presence of 2-PrOH as solvent/H-donor exhibited the suppression of the transesterification reaction in the presence of both Pd/ZrO<sub>2</sub> and t-

ZrO<sub>2</sub> catalysts, resulting in a GVL selectivity of 100 % due to the lower tendency of propanol to behave as nucleophile.

Subsequently, our attention shifted to examining the ability of both Pd/ZrO<sub>2</sub> and t-ZrO<sub>2</sub> catalysts in the conversion of limonene (LIM) into p-cymene (CYM). In principle, the envisaged reaction can proceed through three potential routes [33–36], as depicted in Scheme 2:

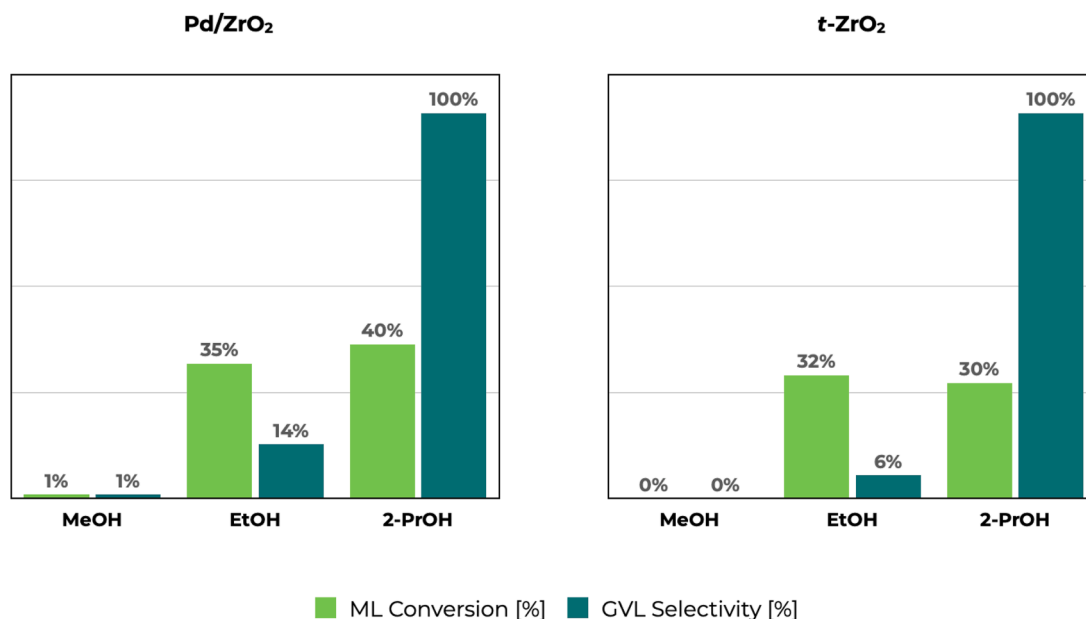
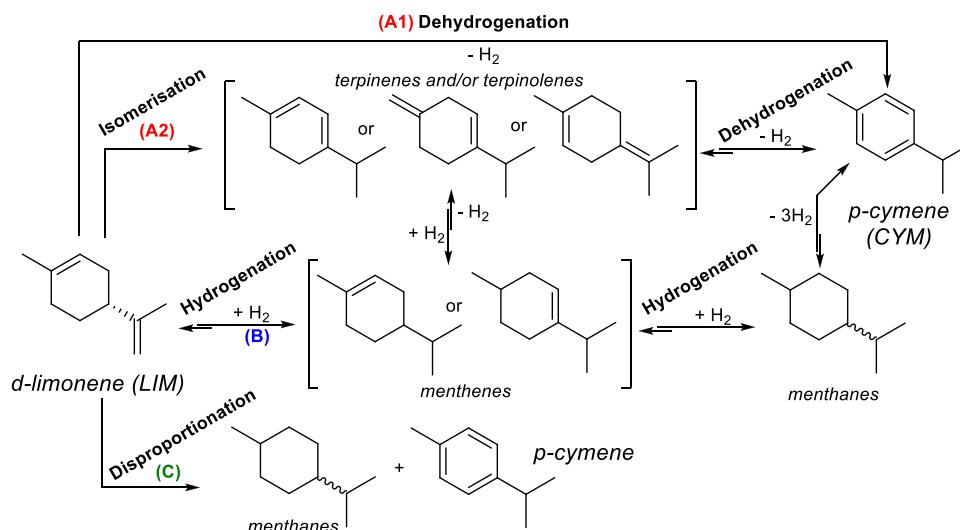


Fig. 3. Transfer hydrogenation of ML into GVL promoted in the presence of Pd/ZrO<sub>2</sub> or t-ZrO<sub>2</sub> catalyst in pure alcoholic H-donor solvents at 250 °C [reaction conditions: 40 mL of 10% wt methyl levulinate solution in MeOH, EtOH or 2-PrOH; 0.2 g of catalyst; initial N<sub>2</sub> pressure: 10 bar; reaction temperature: 250 °C; speed stirring: 500 rpm].



**Scheme 2.** Simplified reaction scheme of the conversion of limonene (LIM) into *p*-cymene (CYM).

- Route A (dehydrogenation): (A1) the direct dehydrogenation of limonene, yielding *p*-cymene or (A2) the isomerization of limonene to terpinenes and terpinolenes, followed by subsequent dehydroaromatization to form *p*-cymene.
- Route B (hydrogenation/dehydrogenation): the previous hydrogenation of limonene results in the formation of menthenes and menthanes, with subsequent dehydroaromatization leading to *p*-cymene.
- Route C (disproportionation): the transformation of limonene into *p*-cymene and methane, accompanied by the generation of *p*-menthene and/or *p*-cymenyl as side-products.

It is not trivial to elucidate a clear mechanism that discriminates among these routes, however the identification of isomerization compounds, such as terpinenes and terpinolenes, or hydrogenation products like menthenes and menthanes in the reaction products, provides substantial support for the first two proposed mechanisms (i.e. isomerization-dehydrogenation and hydrogenation-dehydrogenation

routes). In any case, it is worth emphasizing that - under the reaction conditions employed - the conversion of LIM to CYM is nontrivial, primarily owing to the presence of the hydrogen-donor solvent, which may preferentially promote the generation of hydrogenated compounds.

The conversion of LIM to CYM was investigated in the range of 200–300 °C maintaining constant the reaction time of 180 min (Fig. 4). Very high LIM conversions can be easily achieved for all investigated reaction temperatures. At 200 °C the fractions of hydrogenated compounds (menthenes and menthanes) are prevalent while at higher temperatures, the selectivity is progressively oriented towards the formation of *p*-cymene, in accordance with the formation of this product resulting from an endothermic, dehydrogenation reaction. The high selectivity in menthenes (MTE) and menthanes (MTA) suggest that the production of cymene mainly occurs through the hydrogenation/dehydrogenation route (Route B); in which the hydrogenation step is assisted by the hydrogen-donor solvent (EtOH). At the same time, the detection of terpenes at lower reaction temperatures implies the simultaneous presence, in less extent, of the isomerization-dehydrogenation pathway (Route A2).

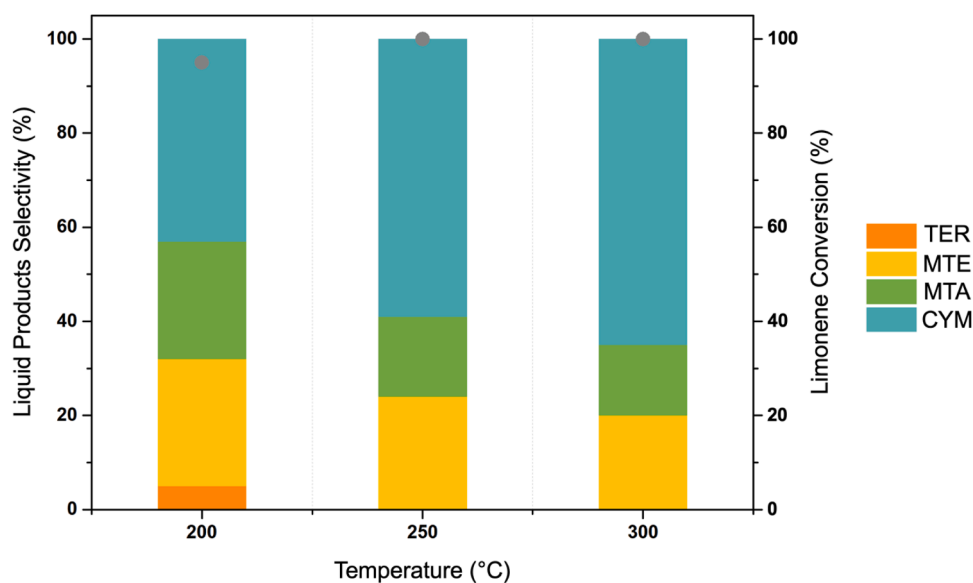


**Fig. 4.** Effect of reaction temperature on the LIM conversion and product selectivity with the Pd/ZrO<sub>2</sub> catalyst under transfer hydrogenation conditions [reaction conditions: 40 mL of LIM solution in EtOH (10% wt); 0.2 g of catalyst; initial N<sub>2</sub> pressure: 10 bar; reaction time: 3 h; speed stirring: 500 rpm].

As expected, in the presence of *t*-ZrO<sub>2</sub> catalyst, no LIM conversion was observed in EtOH under all reaction temperature investigated, implying that the presence of palladium is essential for the dehydrogenation of LIM into CYM.

Subsequently, we proceeded to explore the concurrent valorization of ML and LIM by varying their molar ratios (from 10:90 to 25:75 and 50:50 respectively) in ethanol, in the presence of the Pd/ZrO<sub>2</sub> catalyst at 250 °C for 6 h (Table 3).

The catalytic results clearly demonstrate the achievement of complete limonene conversion across all investigated ML:LIM molar ratios, with minimal deviations in product selectivity that closely resemble those obtained when pure limonene was used as starting substrate.

Noteworthy a reduction in ML conversion with increasing LIM excess is noticeable, particularly evident at the 50:50 molar ratio, leading to a pronounced shift in the formation of ethyl levulinate (EL). This behavior can be rationalized considering a competitive adsorption mechanism between LIM and either ML or EtOH over the Pd nanoparticles, this way hindering the production of GVL. These observations underscore the intricate interplay between reactant ratios and resulting product profiles, providing valuable insights for optimizing the concurrent valorization of ML and LIM, with implications for enhancing overall process efficiency.

#### Catalytic tests under continuous gas-flow conditions

Under continuous, gas flow conditions, the production of  $\gamma$ -valerolactone (GVL) in the presence of a Pd/ZrO<sub>2</sub> catalyst demonstrates exceptional stability compared to the known state of the art [17,18,24]. Indeed, the observed yield remains consistently high, ranging between 60 % and 40 %, sustained for over 55 h of continuous reaction (Fig. 5). It is noteworthy that – in contrast with results obtained under batch conditions – the generally accepted mechanism of the transfer hydrogenation of ML with ethanol performed in the gas-phase is mediated by the rapid formation of AnL (route i, Scheme 1) with consecutive reduction to GVL. Interestingly, under these conditions and over the fresh catalyst, also considerable amount of EPA, between 20 and 30 %, was produced. This can be explained either through the GVL esterification with ethanol toward ethyl 4-hydroxypentanoate or via the direct reduction of ML (or EL) carbonyl toward the hydroxy-esters. In both cases, the latter rapidly undergoes to dehydration reaction under the adopted reaction conditions, leading to EPE which are effectively and selectively transformed into their respective EPA thanks to the presence of the supported Pd nanoparticles which enhance ethanol dehydrogenation to acetaldehyde, therefore promoting hydrogen activation for the hydrogenation of EPE double bond.

On the contrary, experiments conducted with the bare *t*-ZrO<sub>2</sub> catalyst (Fig. 6) revealed a comparatively shorter catalyst lifetime in contrast to those utilizing Pd/ZrO<sub>2</sub> together with the formation of considerable amount of EPE. The obtained results clearly highlight:

- the enhanced durability achieved through the incorporation of a minimal amount of palladium, underlined by both the sharper decrease of ML conversion from 100 % to 95 % and the concomitant increase of EL yield to 30 % at shorter reaction time (i.e. 14 h vs 35 h), in the case of the bare *t*-ZrO<sub>2</sub>;
- the absence of EPA and the concomitant increase of EPE selectivity clearly showing the role of Pd in the reduction of EPE double bond, excluding a more conventional CTH mechanism over the zirconia surface;
- the formation of similar amount of EPE compared to the EPA obtained over Pd/ZrO<sub>2</sub> suggesting that GVL alcoholysis to ethyl 4-hydroxypentanoate and the consecutive dehydration of the latter is the main responsible for EPE formation.

A consistent and thorough conversion of LIM is attainable through the utilization of a Pd/ZrO<sub>2</sub> catalyst, showcasing notable selectivity towards CYM, as depicted in Fig. 7. Significantly, a strong correlation between CYM and H<sub>2</sub> yields has been established, providing compelling evidence for the isomerization-dehydrogenation pathway. In general terms, the employment of ethanol as a diluting agent proves effective in curtailing unwanted oligomerization reactions, ultimately enhancing the molar balances of the process (Fig. 8). Not surprisingly, *t*-ZrO<sub>2</sub> exhibits no distinctive dehydrogenating properties, primarily facilitating LIM isomerization and disproportionation mechanisms, resulting in a 1:1 ratio of CYM and MTE with an approximate yield of 10% mol each. Additionally, TER is formed with a yield of approximately 15 %. Nevertheless, a significant portion of LIM remains unreacted, accumulating on the catalyst's surface, thereby contributing to suboptimal molar balances, as illustrated in Fig. 9.

On the other hand, when we tried to couple the two target reactions (i.e. LIM dehydrogenation to CYM and ML reduction to GVL) over Pd/ZrO<sub>2</sub> a stable and complete conversions of both substrates were achieved for 18 h of time on stream (Fig. 10). However, while a good CYM yield was observed (from 92 to 80 %), an insignificant production of ML related compounds was noted, meaning that some parasite oligomerisation reactions occur. Considering the well-known, efficient, intramolecular cyclisation of ML to AnL over ZrO<sub>2</sub> based catalyst in the gas phase, together with the high AnL tendency to undergoes oligomerisation catalysed by both basic and acid sites [37,38], the most probable explanation of this behaviour is linked with oligomerisation reactions between AnL and LIM derived compounds over the catalyst surface. An additional, indirect confirmation of this can be found in the molar balance of LIM, which is around 80 % on a steady state regime, meaning a loss of LIM which is in good agreement with the LIM:ML molar ratio equal to 5 used in the feed.

To limit the extent of these parasite oligomerisation reactions we also tried to increase the feed dilution shifting from 1% mol to 0.1% mol of the organic mixture in N<sub>2</sub> however without any kind of improvements in GVL production.

## Conclusion

In this contribution, the ability of Pd/ZrO<sub>2</sub> and *t*-ZrO<sub>2</sub> catalysts in the (concurrent) dehydrogenation of limonene into *p*-cymene and the transfer hydrogenation of methyl levulinate into  $\gamma$ -valerolactone has been investigated under both batch and continuous gas-flow conditions with the aim to highlights the circular economy potential of utilizing OPW-derived feedstocks in catalytic processes.

Under batch conditions, the Pd/ZrO<sub>2</sub> catalyst exhibited good performance in the transfer hydrogenation of methyl levulinate (ML) with ethanol as the hydrogen source, achieving substantial ML conversion (73 %) at 300 °C with a GVL yield of 24 %. Lower temperatures resulted in decreased conversions and notable shifts in product selectivity due to the increased tendency of ML to undergo transesterification. The time effect analysis at 250 °C revealed a progressive increase in ML

**Table 3**

Concurrent catalytic conversion of methyl levulinate (ML) and limonene (LIM) by varying their molar ratios (10:90 - 25:75 - 50:50) in the presence of Pd/ZrO<sub>2</sub> catalyst by using ethanol as H-source at 250 °C for 6 h. ML+LIM overall amount was equal to 10 %wt in ethanol.

ML-LIM molar ratio	ML Conv. [%]	ML products selectivity [%]		LIM Conv. [%]	LIM products selectivity [%]		
		GVL	EL		MTE	MTA	CYM
10:90	100	57	43	100	35	10	55
25:75	90	48	52	100	32	11	57
50:50	40	37	63	100	30	11	59

ML: Methyl Levulinate; LIM: Limonene; GVL:  $\gamma$ -valerolactone; EL: ethyl levulinate; MTE: menthenes; MTA: menthanes.

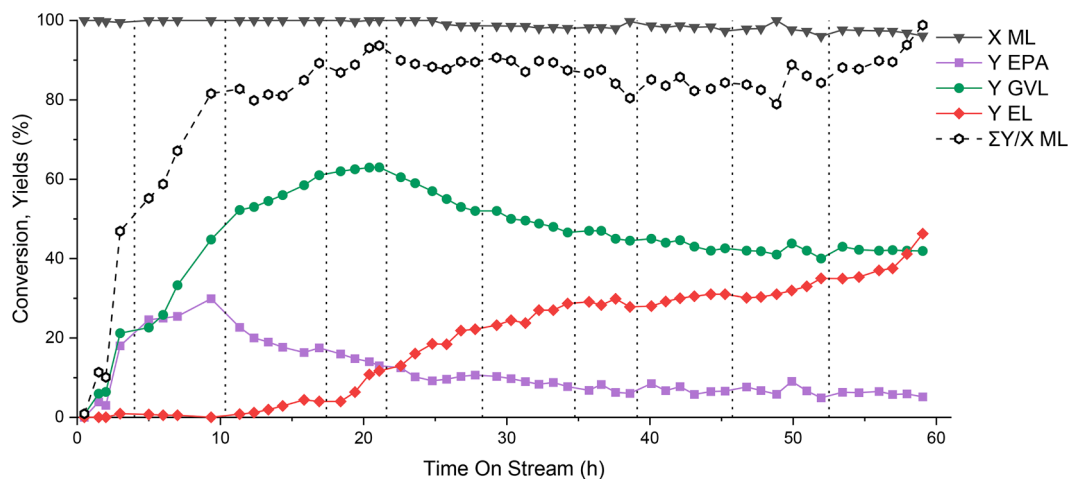


Fig. 5. CTH of ML with ethanol over Pd/ZrO<sub>2</sub>. Reaction conditions: ML:EtOH molar ratio equal to 1:10; T = 250 °C; τ = 1 s; %vol org = 9 % in N<sub>2</sub>.

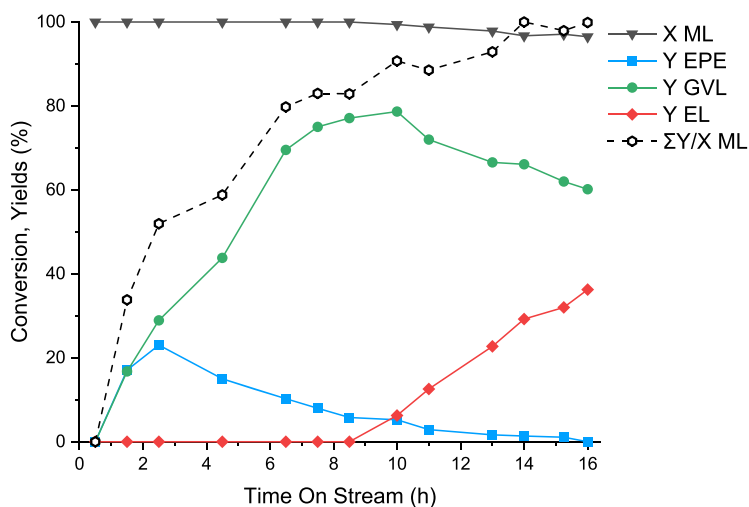


Fig. 6. CTH of ML with ethanol over t-ZrO<sub>2</sub>. Reaction conditions: ML:EtOH molar ratio equal to 1:10; T = 250 °C; τ = 1 s; %vol org = 8 % in N<sub>2</sub>.

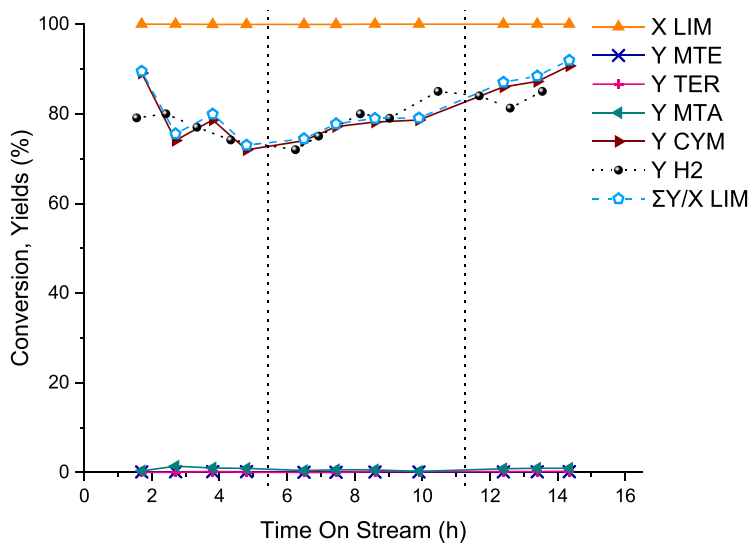


Fig. 7. Conversion of neat LIM to CYM over Pd/ZrO<sub>2</sub>. Reaction conditions: T = 250 °C; τ = 1 s; %vol org = 1 % in N<sub>2</sub>.



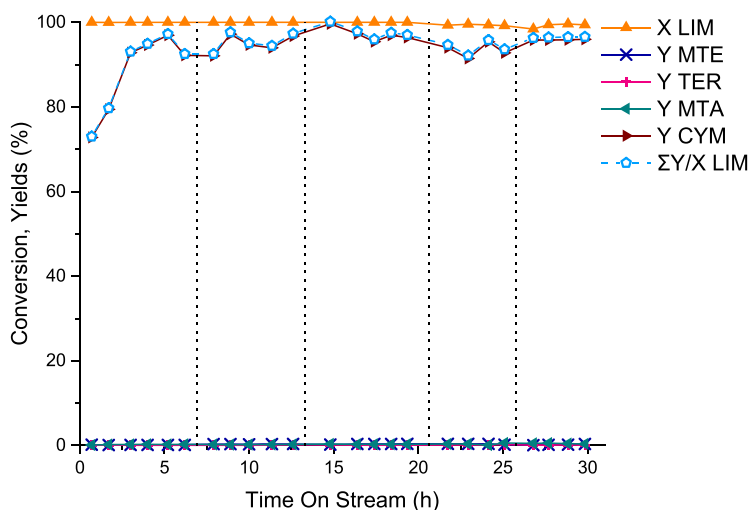


Fig. 8. Conversion of LIM to CYM over Pd/ZrO<sub>2</sub> in presence of ethanol. LIM:EtOH molar ratio equal to 1:10;  $T = 250\text{ }^{\circ}\text{C}$ ;  $\tau = 1\text{ s}$ ; %vol org = 9 % in N<sub>2</sub>.

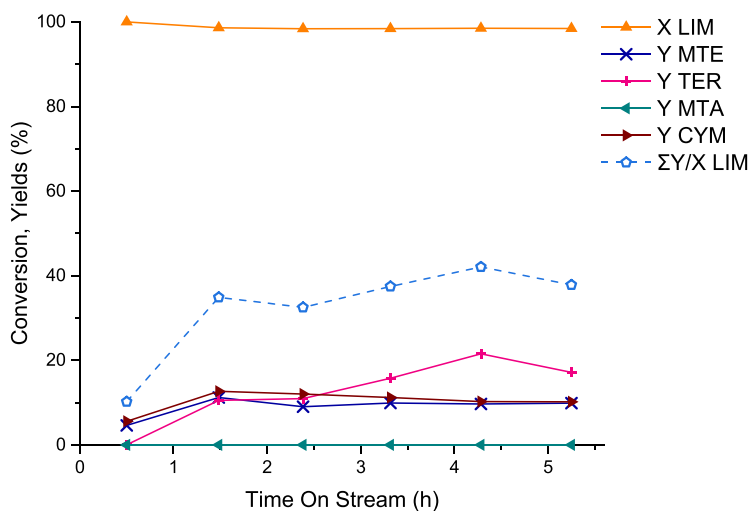


Fig. 9. Conversion of neat LIM to CYM over *t*-ZrO<sub>2</sub>. Reaction conditions:  $T = 250\text{ }^{\circ}\text{C}$ ;  $\tau = 1\text{ s}$ ; %vol org = 1 % in N<sub>2</sub>.

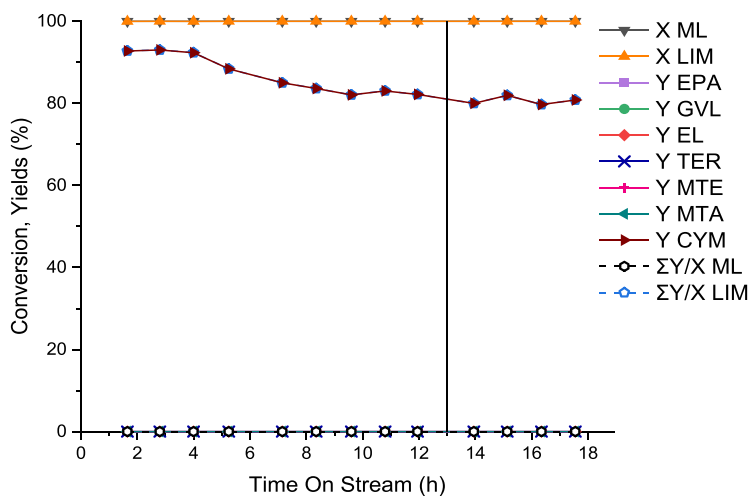


Fig. 10. Conversion of a mixture of ML and LIM over Pd/ZrO<sub>2</sub>. Reaction conditions: ML:LIM molar ratio equal to 1:5;  $T = 250\text{ }^{\circ}\text{C}$ ;  $\tau = 1\text{ s}$ ; %vol org = 1 % in N<sub>2</sub> for the first 12 h on stream (left of the break); %vol org = 0.1 % in N<sub>2</sub> from the 14th h on stream (right of the break).

conversion with Pd/ZrO<sub>2</sub>, reaching 68 % after 24 h, highlighting the catalyst's effectiveness in promoting transfer hydrogenation over transesterification. The choice of solvent/H-donor also played a crucial role, with ethanol proving to be more effective than methanol, and 2-propanol suppressing transesterification, leading to 100 % GVL selectivity. The catalyst's ability to convert limonene (LIM) into *p*-cymene (CYM) revealed a high selectivity for CYM formation, primarily through the hydrogenation/dehydrogenation route. The concurrent catalytic conversion of ML and LIM using Pd/ZrO<sub>2</sub> catalyst showcased complete LIM conversion across various ML:LIM ratios, with product selectivity closely resembling that of pure LIM. The study under continuous gas-flow conditions demonstrated exceptional stability in GVL production with Pd/ZrO<sub>2</sub>, sustaining yields between 60 % and 40 % over 50 h.

Comparatively, the bare ZrO<sub>2</sub> catalyst showed a shorter lifespan, emphasizing the enhanced durability achieved by incorporating palladium. Very high conversion of LIM was registered with a strong correlation between CYM and H<sub>2</sub> yields, compelling evidence has been provided for the isomerization-dehydrogenation pathway.

The catalytic investigation of the simultaneous upgrading of ML and LIM over Pd/ZrO<sub>2</sub> revealed stable and complete conversions for 18 h, with surprisingly low production of ML-related compounds. This behavior was attributed to oligomerization/Diels Alder reactions between angelica lactone and LIM-derived compounds over the catalyst surface.

## Fundings

Project Ecosistema TECH4YOU – Technologies for climate change adaptation and quality of life improvement (PNRR MUR - M4C2 - Investimento 1.5 - "Ecosistemi dell'Innovazione"), Spoke 3 - Goal 3.5 is acknowledged for the financial support.

## CRediT authorship contribution statement

**A. Allegri:** Conceptualization, Methodology, Investigation, Writing – original draft. **E. Paone:** Conceptualization, Supervision, Methodology, Investigation, Writing – original draft. **C. Bosticco:** Methodology, Investigation. **A. Pedullà:** Methodology, Investigation. **M.G. Musolino:** Supervision, Writing – original draft, Funding acquisition. **F. Cavani:** Conceptualization, Supervision, Writing – original draft, Funding acquisition. **T. Tabanelli:** Conceptualization, Methodology, Investigation, Funding acquisition. **S. Albonetti:** Conceptualization, Supervision, Writing – original draft, Funding acquisition.

## Declaration of competing interest

The authors declare that they have no known competing financial interests or personal relationships that could have appeared to influence the work reported in this paper.

## Data availability

Data will be made available on request.

## Acknowledgments

This paper is dedicated to the memory of Prof. Rosario Pietropaolo that unexpectedly passed away on July 1st, 2022. Rector of the Università degli Studi Mediterranea di Reggio Calabria, first Dean of the Faculty of Engineering as well as a visionary of science, master of ethics, integrity and dedication and inspiration for many colleagues and students. Emilia Paone gratefully acknowledges the Italian Ministry for University and Research (MUR) and the Università degli Studi Mediterranea di Reggio Calabria for funding under D.M. 1062/2021 and D.M. 737/2022 programs. Prof. Maria Grazia Musolino gratefully

acknowledges the Italian Ministry for University and Research (MUR) for funding within the project Ecosistema TECH4YOU – Technologies for climate change adaptation and quality of life improvement (PNRR MUR - M4C2 - Investimento 1.5 - "Ecosistemi dell'Innovazione"). Dr. Tommaso Tabanelli is grateful to Italian Ministry for University and Research (MUR) for the financial support provided through the PRIN 2020 LEVANTE project "LEvulinic acid Valorization through Advanced Novel Technologies" (Progetti di Ricerca di Rilevante Interesse Nazionale-Bando 2020, 2020CZCJN7).

## References

- [1] M. Besson, P. Gallezot, C. Pinel, Conversion of biomass into chemicals over metal catalysts, *Chem. Rev.* 114 (2014) 1827–1870.
- [2] C. Xu, E. Paone, D. Rodríguez-Pradrón, R. Luque, F. Mauriello, Recent catalytic routes for the preparation and the upgrading of biomass derived furfural and 5-hydroxymethylfurfural, *Chem. Soc. Rev.* 49 (2020) 4273–4306.
- [3] C. Espro, E. Paone, F. Mauriello, R. Gotti, E. Uliassi, M.L. Bolognesi, D. Rodríguez-Pradrón, R. Luque, Sustainable production of pharmaceutical, nutraceutical and bioactive compounds from biomass and waste, *Chem. Soc. Rev.* 50 (2021) 11191–11207.
- [4] FAO, Citrus Fruit Fresh and Processed Statistical Bulletin 2020, Food and Agriculture Organization of the United Nations, 2021 [, <https://www.fao.org/3/cb6492en/cb6492en.pdf>].
- [5] United States Department of Agriculture, Citrus: World Markets and Trade, Foreign Agricultural Service, Washington, DC, USA, 2019.
- [6] N. Mahato, M. Sinha, K. Sharma, R. Koteswararao, M.H. Cho, Modern extraction and purification techniques for obtaining high purity food-grade bioactive compounds and value-added co-products from citrus wastes, *Foods* 8 (2019) 1–81.
- [7] A. Satira, E. Paone, V. Bressi, D. Iannazzo, F. Marra, P.S. Calabrò, F. Mauriello, C. Espro, Hydrothermal carbonization as sustainable process for the complete upgrading of orange peel waste into value-added chemicals and bio-carbon materials, *Appl. Sci.* 11 (2021) 10983.
- [8] P.S. Calabrò, E. Paone, D. Komilis, Strategies for the sustainable management of orange peel waste through anaerobic digestion, *J. Environ. Manag.* 212 (2018) 462–468.
- [9] A.S. Matharu, E.M. de Melo, J.A. Houghton, Opportunity for high value-added chemicals from food supply chain wastes, *Bioresour. Technol.* 215 (2016) 123–130.
- [10] F. Meneguzzo, C. Brunetti, A. Fidalgo, R. Ciriminna, R. Delisi, L. Albanese, F. Zabini, A. Gori, L.B. Nascimento, A. De Carlo, F. Ferrini, L.M. Ilharco, M. Pagliaro, Real-scale integral valorization of waste orange peel via hydrodynamic cavitation, *Processes* 7 (2019) 581.
- [11] R. Rinaldi, F. Schüth, Acid hydrolysis of cellulose as the entry point into biorefinery schemes, *ChemSusChem* 2 (2009) 1096–1107.
- [12] D. Ghosh, D. Dasgupta, D. Agrawal, S. Kaul, D. Adhikari, A.K. Kurmi, P.K. Arya, D. Bangwal, M.S. Negi, Fuels and chemicals from lignocellulosic biomass: an integrated biorefinery approach, *Energy Fuels* 29 (2015) 3149–3157.
- [13] A.J. Ayala, G. Montero, M.A. Coronado, C. García, M.A. Curiel-Alvarez, J.A. León, C.A. Sagaste, C. A. D.G. Montes, Characterization of orange peel waste and valorization to obtain reducing sugars, *Molecules* 26 (2021) 1348.
- [14] X. Liang, Y. Fu, J. Chang, Sustainable production of methyl levulinate from biomass in ionic liquid-methanol system with biomass-based catalyst, *Fuel* 259 (2020) 116246.
- [15] L. Negahdar, M.G. Al-Shaal, F.J. Holzhauser, R. Palkovits, Kinetic analysis of the catalytic hydrogenation of alkyl levulinates to  $\gamma$ -valerolactone, *Chem. Eng. Sci.* 158 (2017) 545–551.
- [16] B. Cai, X.C. Zhou, Y.C. Miao, J.Y. Luo, H. Pan, Y.B. Huang, Enhanced catalytic transfer hydrogenation of ethyl levulinate to  $\gamma$ -valerolactone over a robust Cu-Ni bimetallic catalyst, *ACS Sustain. Chem. Eng.* 5 (2017) 1322–1331.
- [17] S. Ostovar, H. Saravani, D. Rodríguez-Pradrón, Versatile functionalized mesoporous Zr/SBA-15 for catalytic transfer hydrogenation and oxidation reactions, *Renew. Energy* 178 (2021) 1070–1083.
- [18] T. Tabanelli, E. Paone, P.B. Vásquez, R. Pietropaolo, F. Cavani, F. Mauriello, Transfer hydrogenation of methyl and ethyl levulinate promoted by a ZrO<sub>2</sub> catalyst: comparison of batch vs continuous gas-flow conditions, *ACS Sustain. Chem. Eng.* 7 (2019) 9937–9947.
- [19] P.B. Vasquez, T. Tabanelli, E. Monti, S. Albonetti, D. Bonincontro, N. Dimitratos, F. Cavani, Gas-phase catalytic transfer hydrogenation of methyl levulinate with ethanol over ZrO<sub>2</sub>, *ACS Sustain. Chem. Eng.* 7 (2019) 8317–8330.
- [20] Gamma valerolactone market size, share, growth, and industry analysis, by type (food grade, industrial grade), by application (food flavors, solvent, monomer intermediate, others) and regional insights and forecast to 2031. *Business Research Inside*. Published 2023.
- [21] T. Tabanelli, S. Passeri, S. Guidetti, F. Cavani, C. Lucarelli, F. Cargnoni, M. Mella, A cascade mechanism for a simple reaction: the gas-phase methylation of phenol with methanol, *J. Catal.* 370 (2019) 447–460.
- [22] T. Tabanelli, Unrevealing the hidden link between sustainable alkylation and hydrogen transfer processes with alcohols, *Curr. Opin. Green Sustain. Chem.* 29 (2021) 100449.
- [23] J. De Maron, M. Eberle, F. Cavani, F. Basile, N. Dimitratos, P.J. Maireles-Torres, E. Rodríguez-Castellón, T. Tabanelli, Continuous-flow methyl methacrylate

- synthesis over gallium-based bifunctional catalysts, *ACS Sustain. Chem. Eng.* 9 (4) (2021) 1790–1803.
- [24] R. Bacchionchi, A. Ventimiglia, A. Canciani, G. Peroni, T. Tabanelli, S. Albonetti, N. Dimitratos, I. Rivalta, S. Zainal, L. Forster, C. D'Agostino, F. Cavani, Structure-activity relationships of ZrO<sub>2</sub> crystalline phases in the catalytic transfer hydrogenation of methyl levulinate with ethanol, *J. Catal.* 428 (2023) 115177.
- [25] M.J. Gilkey, B. Xu, Heterogeneous catalytic transfer hydrogenation as an effective pathway in biomass upgrading, *ACS Catal.* 6 (2016) 1420–1436.
- [26] C. Espro, B. Gumina T. Szumelda, E. Paone, F. Mauriello, Catalytic transfer hydrogenolysis as an effective tool for the reductive upgrading of cellulose, hemicellulose, lignin, and their derived molecules, *Catalysts* 8 (2018) 313.
- [27] J. Zhang, C. Zhao, A new approach for bio-jet fuel generation from palm oil and limonene in the absence of hydrogen, *Chem. Commun.* 51 (2015) 17249–17252.
- [28] J. Zhang, C. Zhao, Development of a bimetallic Pd-Ni/HZSM-5 catalyst for the tandem limonene dehydrogenation and fatty acid deoxygenation to alkanes and arenes for use as biojet fuel, *ACS Catal.* 6 (2016) 4512–4525.
- [29] G.K. Chuah, S. Jaenicke, S.A. Cheong, K.S. Chan, The influence of preparation conditions on the surface area of zirconia, *Appl. Catal. A* 145 (1–2) (1996) 267–284.
- [30] K. Pokrovski, K.T. Jung, A. Bell, Investigation of CO and CO<sub>2</sub> adsorption on tetragonal and monoclinic zirconia, *Langmuir* 17 (2001) 4297–4303.
- [31] S. Wang, E. Iglesia, Experimental and theoretical evidence for the reactivity of bound intermediates in ketonization of carboxylic acids and consequences of acid–base properties of oxide catalysts, *J. Phys. Chem. C* 121 (2017) 18030–18046.
- [32] J. De Maron, L. Bellotti, A. Baldelli, A. Fasolini, N. Schiaroli, C. Lucarelli, F. Cavani, T. Tabanelli, Evaluation of the catalytic activity of metal phosphates and related oxides in the ketonization of propionic acid, *Sustain. Chem.* 2 (2022) 58–75.
- [33] D. Zhao, T. Su, D. Rodríguez-Padron, H. Lü, C. Len, R. Luque, Z. Yang, Efficient transfer hydrogenation of alkyl levulinates to g-valerolactone catalyzed by simple Zr-TiO<sub>2</sub> metal oxide systems, *Mater. Today Chem.* 24 (2022) 100745.
- [34] X. Tang, L. Hu, Y. Sun, G. Zhao, W. Hao, L. Lin, Conversion of biomass-derived ethyl levulinate into g-valerolactone via hydrogen transfer from supercritical ethanol over a ZrO<sub>2</sub> catalyst, *RSC Adv.* 3 (2013) 10277–10284.
- [35] D. Makarouni, S. Lycourghiotis, E. Kordouli, K. Bourikas, C. Kordulis, V. Dourtoglou, Transformation of limonene into p-cymene over acid activated natural mordenite utilizing atmospheric oxygen as a green oxidant: a novel mechanism, *Appl. Catal. B Environ.* 224 (2018) 740–750.
- [36] M. Kamitsou, G.D. Panagiotou, K.S. Triantafyllidis, K. Bourikas, A. Lycourghiotis, C. Kordulis, Transformation of -limonene into p-cymene over oxide catalysts: a green chemistry approach, *Appl. Catal. A Gen.* 474 (2014) 224–229.
- [37] D. Sun, Y. Takahashi, Y. Yamada, S. Sato, Efficient formation of angelica lactones in a vapor-phase conversion of levulinic acid, *Appl. Catal. A Gen.* 526 (2016) 62–69.
- [38] M. Mascal, S. Dutta, I. Gandarias, Hydrodeoxygenation of the angelica lactone dimer, a cellulose-based feedstock: simple, high-yield synthesis of branched C7-C10 gasoline-like hydrocarbons, *Angew. Chem. Int. Ed.* 53 (2014) 1854–1857.